Saturn's Variable Thermosphere Part 2

By
Darrell F. Strobel
strobel @ jhu.edu
Johns Hopkins University, Baltimore, MD 21218, U.S.A.

Tommi Koskinen
Lunar and Planetary Laboratory, University of Arizona, Tucson, AZ 85721-0092

Ingo Müller-Wodarg
Blackett Laboratory, Imperial College, London, UK

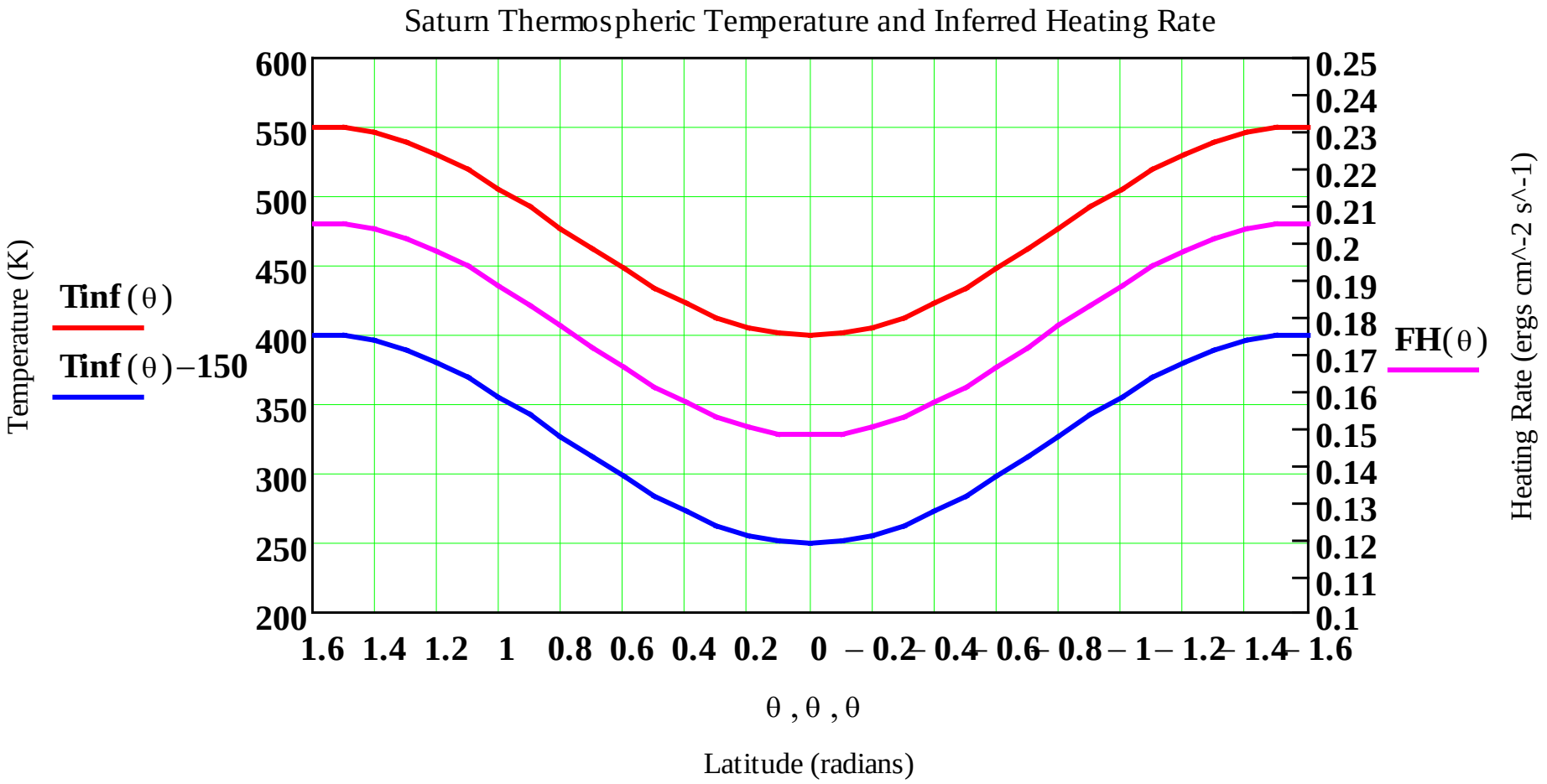

$$Let\ T_\infty(\theta) = 550 - 150\cos^2(\theta);\ Assume\ F_H(\theta) \propto T_\infty(\theta)$$

Globally averaged, inferred column heating rate FH = 0.17 ergs cm^{-2} s^{-1} or 7.6 TW total for Saturn

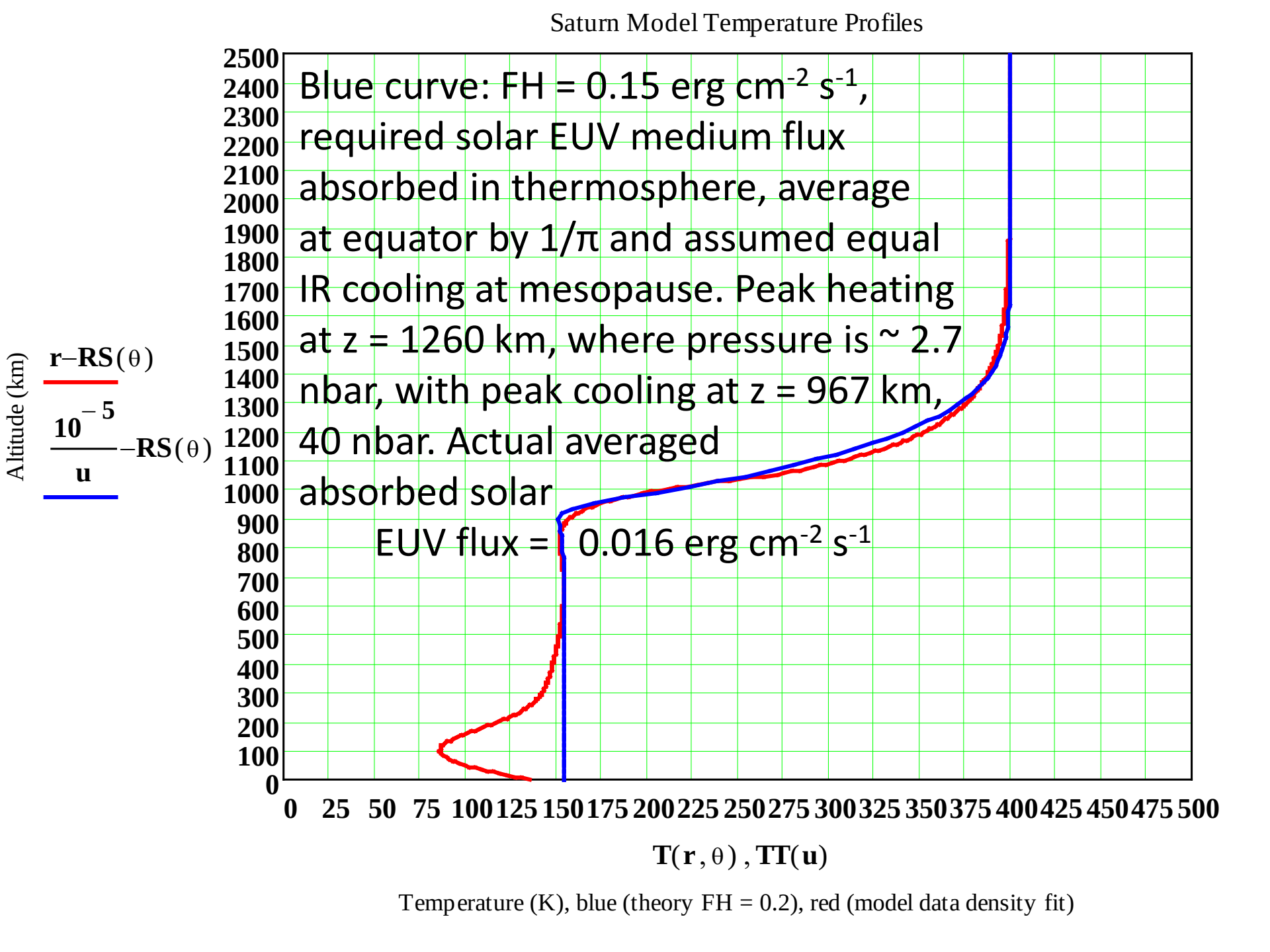
Saturn Model Temperature Profiles
Blue curve: FH = 0.15 erg cm-2 s-1, required solar EUV medium flux absorbed in thermosphere, average at equator by 1/π and assumed equal IR cooling at mesopause. Peak heating at z = 1260 km, where pressure is ~ 2.7 nbar, with peak cooling at z = 967 km, 40 nbar. Actual averaged absorbed solar EUV flux = 0.016 erg cm-2 s-1
Altitude (km)
r–RS(θ)
10^−5 / u –RS(θ)
2500 2400 2300 2200 2100 2000 1900 1800 1700 1600 1500 1400 1300 1200 1100 1000 900 800 700 600 500 400 300 200 100 0
0 25 50 75 100 125 150 175 200 225 250 275 300 325 350 375 400 425 450 475 500
T(r, θ) , TT(u)
Temperature (K), blue (theory FH = 0.2), red (model data density fit)

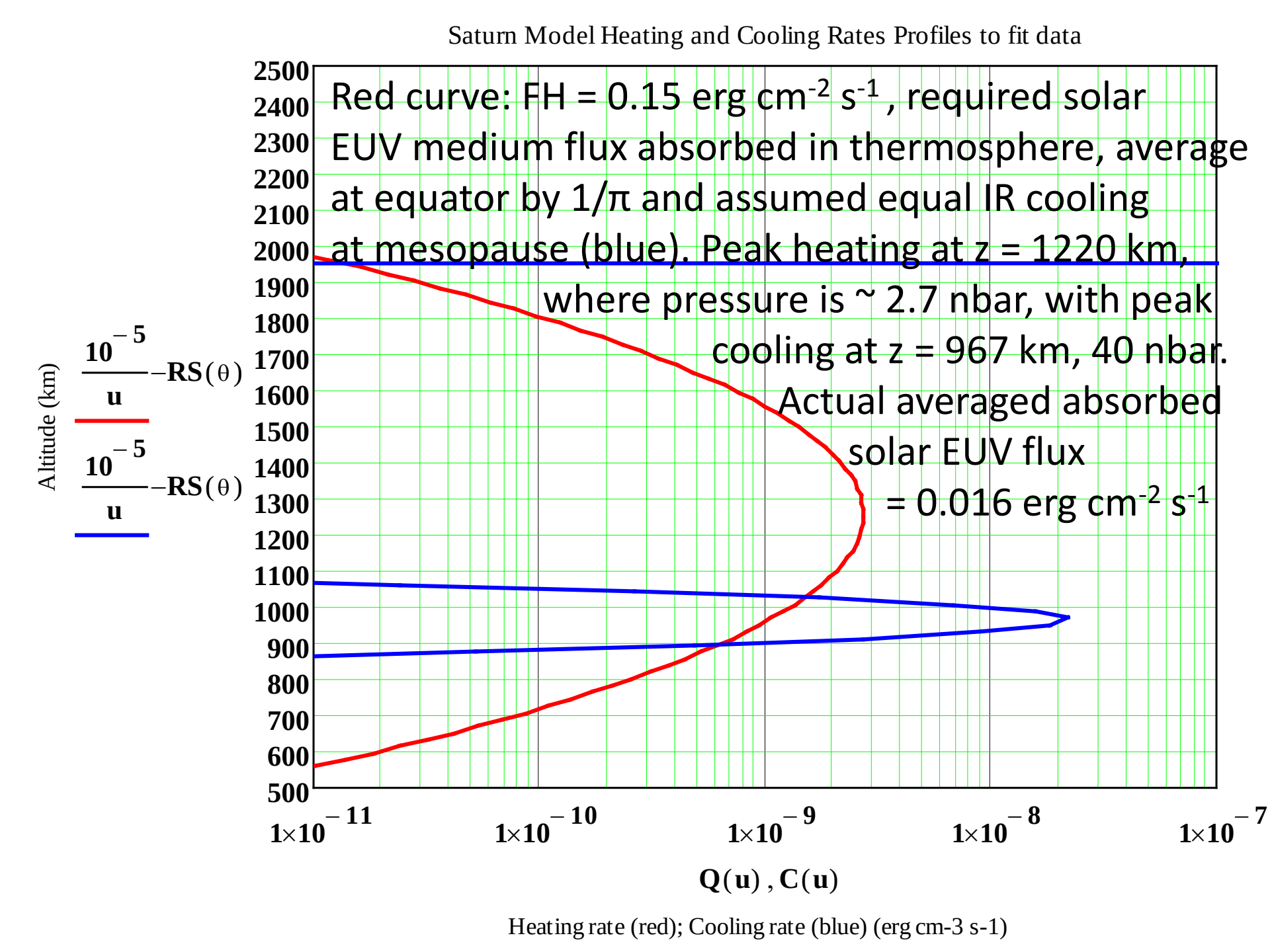
Saturn Model Heating and Cooling Rates Profiles to fit data
Red curve: FH = 0.15 erg cm-2 s-1 , required solar EUV medium flux absorbed in thermosphere, average at equator by 1/π and assumed equal IR cooling at mesopause (blue). Peak heating at z = 1220 km, where pressure is ~ 2.7 nbar, with peak cooling at z = 967 km, 40 nbar. Actual averaged absorbed solar EUV flux = 0.016 erg cm-2 s-1
Altitude (km)
10^-5 / u − RS(θ)
10^-5 / u − RS(θ)
2500
2400
2300
2200
2100
2000
1900
1800
1700
1600
1500
1400
1300
1200
1100
1000
900
800
700
600
500
1×10^-11
1×10^-10
1×10^-9
1×10^-8
1×10^-7
Q(u) , C(u)
Heating rate (red); Cooling rate (blue) (erg cm-3 s-1)

Summary of Thermospheric Power Sources and Inferred Heating Rates

Planet	λ_0	T_∞ (K)	$\lambda_{exobase}$	$r_{exobase}/r_p$	Composition
Saturn	1300	400-550	420	1	H_2, He

Quantity (TW)	Jupiter	Saturn
Solar UV Input	2.4	0.73
Particle Power Input	30	0.2
Joule Heating	1,000	10
Inferred Total Heating Rate	35	7.6
Maximum Gravity Wave Power (heating)	27	6 (2.4)

Joule/Ion-neutral heating rate (column integrated)

$$Q_J = \frac{1}{\rho}\mathbf{J}\cdot\mathbf{E} = \frac{1}{\rho}\sigma\left(\mathbf{E}+\mathbf{u}\times\mathbf{B}\right)\cdot\mathbf{E}$$

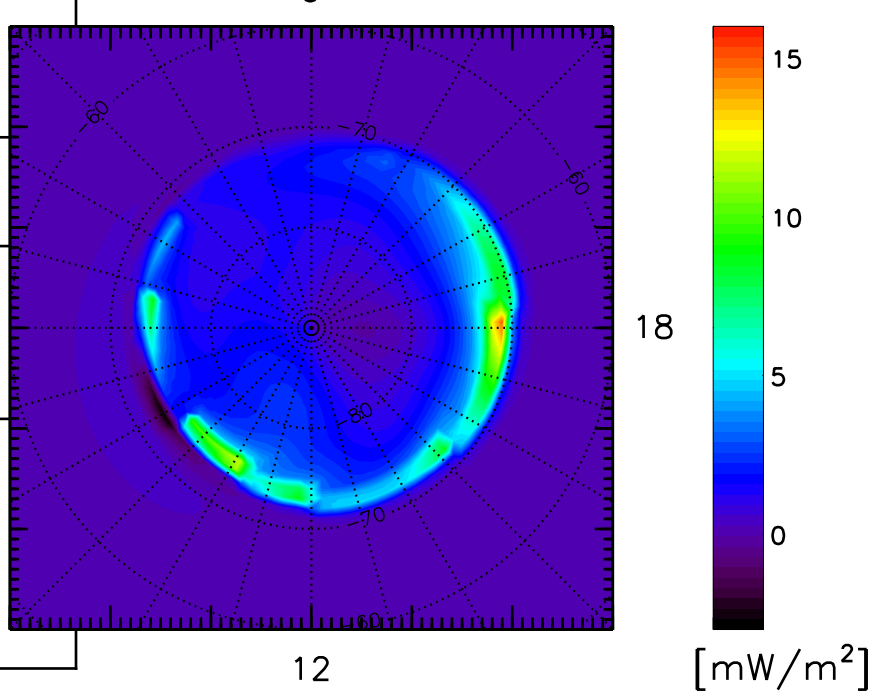

Global heating rates: EUV: 0.6, Joule: 5.8 TW

Gravity Waves in Planetary Atmospheres

Angular frequency: $\omega = k_h c$, where c = zonal phase speed and k_h = zonal wavenumber

Intrinsic/Doppler shifted angular frequency: $\omega = k_h(c - u)$, where u = mean zonal wind

Coriolis parameter: $f = 2 \cdot \Omega \cdot \sin(\mathrm{Lat})$ **Ω = rotation rate of planet**

Buoyancy or Brunt-Vaisalla frequency: $$N = \left[\frac{g}{T} \cdot \left(\frac{dT}{dz} + \frac{g}{c_p} \right) \right]^{0.5}$$

Zonal horizontal wavelength = $\lambda_h = 2\pi/k_h$ **Vertical wavelength, $\lambda_z = 2\pi/k_z$**

Meridional horizontal wavelength = $\lambda_y = 2\pi/l$

Density scale height = H_d

Aspect ratio: $$\delta = \left[1 + \left(\frac{\lambda_h}{\lambda_y} \right)^2 \right]^{0.5}$$

General dispersion relation for gravity waves: $$k_z = \left[\left(\frac{N^2 - \omega^2}{\omega^2 - f^2} \right) \cdot (k_h)^2 \cdot \delta^2 - \frac{1 - 2 \cdot \frac{dH_d}{dz}}{4 \cdot (H_d)^2} \right]^{0.5}$$

and for hydrostatic gravity waves: $H_d k_h^2 (u-c)^2 / g \ll 1$, which is equivalent to $\omega^2 \ll N^2$

$$k_z = \left[\left(\frac{\delta \cdot N}{u - c} \right)^2 - (k_h)^2 \cdot \delta^2 - \frac{1}{4 \cdot (H_d)^2} \right]^{0.5}$$

and with the "Boussinesq" approximation, $k_z^2 \gg 1 / 4H_d^2$, the last term in k_z is negligible.

Vertical transfer of energy & momentum by gravity waves requires, c_g = group velocity

$$\frac{c_{gz}}{c_{gh}} = \frac{\left(\omega^2 - f^2\right)^{0.5}}{N}$$

~ k_h/k_z, should not be too small or most gravity wave energy will be dispersed horizontally and this implies $\omega^2 >> f^2$

Eliassen-Palm flux: $F = c_{gz} A$

$$c_{gz} = \frac{N \cdot k_h}{\left(k_z\right)^2} \qquad A = -k_h \cdot \left(\frac{E}{\omega - k_h u}\right)$$

Total wave energy (energy density):

$$E = \frac{1}{2} \cdot \rho_0 \cdot \left[\left(u_p\right)^2 + \left(v_p\right)^2 + \left(w_p\right)^2 + \frac{N^2 \cdot \left(w_p\right)^2}{\left(k_h\right)^2 \cdot (u - c)^2} \right]$$

Wave saturation criteria:

$$\left|\frac{dT_0}{dz}\right| + \left(\left|\frac{dT_p}{dz}\right|\right)_{sat} \geq \frac{g}{c_p} \qquad \left(T_p\right)_{sat} \geq \frac{N^2 \cdot T_0}{g \cdot k_z}$$

$$\left(u_p\right)_{sat} \geq \left|u - c\right|$$

$$\left(\left|w_p\right|\right)_{sat} \geq c_{gz} = \frac{k_h \cdot \left|u - c\right|}{k_z}$$

In the thermosphere molecular viscosity, μ, acts to dissipate the wave energy with the wave reaching a maximum amplitude at the level where wave dissipation cancels exponential $(\rho_0)^{-0.5}$ amplitude growth

$$k_{zi} = \frac{1}{2 \cdot H_d} \quad \text{, where} \quad k_{zi} = \frac{k_{zr}}{2}\left(\frac{\omega_i}{\omega_r}\right)\cdot\left(1+\frac{1}{Pr}\right) = 1.22\cdot\frac{\mu}{\rho_0}\cdot\frac{\left(k_{zr}\right)^3}{\omega_r}$$

where the Prandtl number, Pr, = 0.69, & the mass density of the atmosphere, ρ_q, where the gravity wave reaches peak amplitude is:

$$\rho_q = H_d \cdot \mu \cdot \frac{\left(k_{zr}\right)^4}{N \cdot k_h}\cdot\left(1+\frac{1}{Pr}\right)$$

The vertical gravity wave energy flux is: $$F_{Ez} = E \cdot c_{gz} = \frac{1}{2}\cdot\rho_q\cdot\frac{g^2}{N^2}\cdot\left|\frac{\omega_r}{k_{zr}}\right|\cdot\frac{\left(T_p\right)^2}{\left(T_0\right)^2}$$

If the gravity wave's peak amplitude is at its saturation amplitude, then upward vertical energy flux has attained its maximum amplitude for heating the thermosphere, where ρ_q is satisfied. At the altitude where $\rho = \rho_q$, molecular viscosity has dissipated $(1-e^{-1}) = 0.63$ of the energy flux before reaching this altitude. The maximum possible upward energy flux from the "lower" atmosphere is:

$$\left(\left|F_{Ez}\right|\right)_{max} = \frac{e^1}{2}\cdot\rho_q\cdot\frac{N^3\cdot k_h}{\left(k_{zr}\right)^4} = \frac{e^1}{2}\cdot\mu\cdot H_d\cdot N^2\cdot\left(1+\frac{1}{Pr}\right) \quad \text{->} \quad 3.32\cdot\frac{\mu\cdot g\cdot R}{c_p}$$

if T = constant

THERMOSPHERIC GRAVITY WAVE HEATING

- With appropriate values for the input parameters, μ, g, and cp/R, the maximum gravity wave energy fluxes in isothermal region is 0.13 erg cm^{-2} s^{-1}, for Saturn and would be marginal even if 100% of energy flux were converted to heat, because the maximum gravity wave energy flux would have to supplied all the time, everywhere over the entire planet.
- Estimated heating efficiency is $$\varepsilon = \frac{Q_{vis}}{Q_{vis} + Q_{buo}} = \frac{1}{1 + \mathrm{Pr}^{-1}} = 0.41$$
- thus the maximum integrated heating rate would be ~ 0.053 erg cm^{-2} s^{-1}, too low by at least a factor of 3, if wave heating were global and continuous.

Saturn upper atmosphere log density contours (cm^-3)

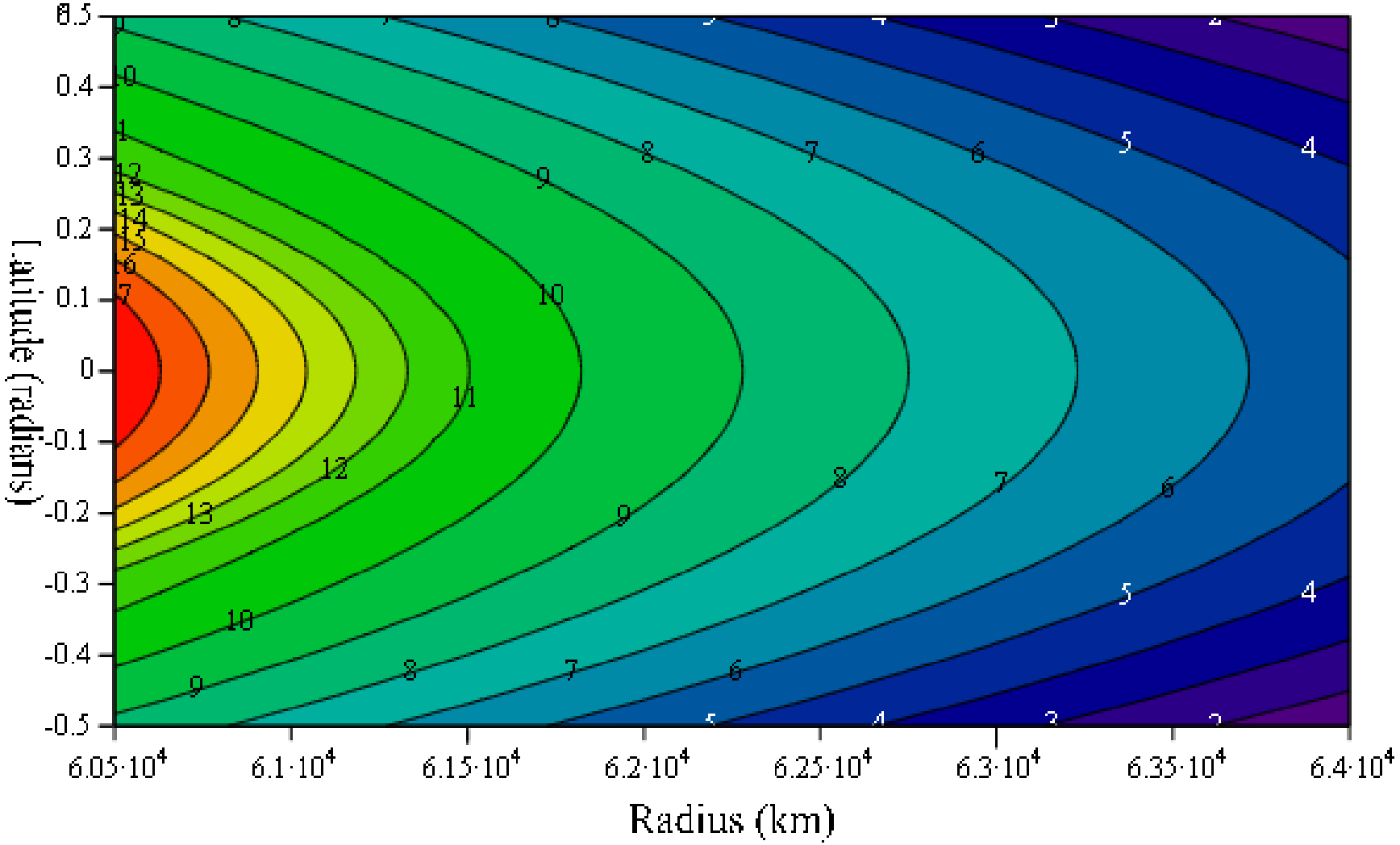

$$n(r,\theta) = n_0 \left\{ \exp[\lambda_0 \cdot (\frac{R_t}{r} - 1)] \right\} \times \exp\left[-\left[43 \sin\left[\left(\frac{\theta}{\Delta\theta} \right)^{-} \right] \right] \right]$$

Dn

$$+ n_0 \left\{ 0.1 \exp\left[-\left(\frac{r - R_t}{H} \right) \right] \right\} \times \exp\left[-\left[200 \sin\left[\left(\frac{\theta}{\Delta\theta} \right)^{2} \right] \right] \right]$$

Note ½ tumble density log 9.882

H_2 cm^{-3} = 2.52 e-11 kg m^{-3}

Rt = 61700 km

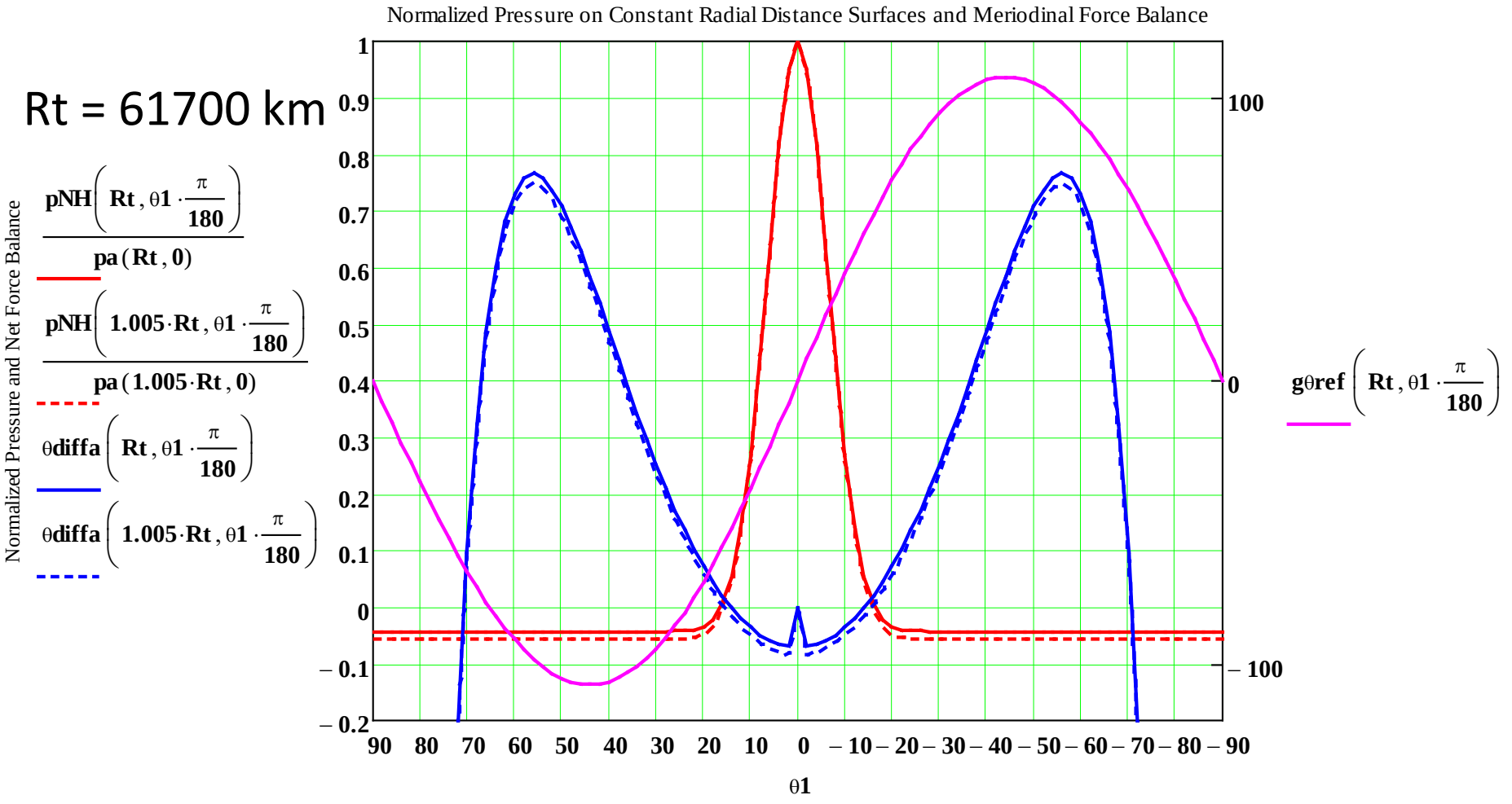

$$\theta\mathbf{diffa}(\mathbf{r},\theta) := \frac{\mathbf{p}\theta\mathbf{a}(\mathbf{r},\theta) - \mathbf{g}\theta\mathbf{ref}(\mathbf{r},\theta)}{\mathbf{g}\theta\mathbf{ref}(\mathbf{r},\theta)}$$

$$\frac{\Delta_{Force}}{Force} = \frac{\frac{1}{\rho r}\frac{\partial p}{\partial \theta} - \frac{1}{r}\frac{\partial \Phi}{\partial \theta}}{\frac{1}{r}\frac{\partial \Phi}{\partial \theta}}; \; \Phi = total \;\; potential \;\; (gravity \,\&\, centrifugal)$$

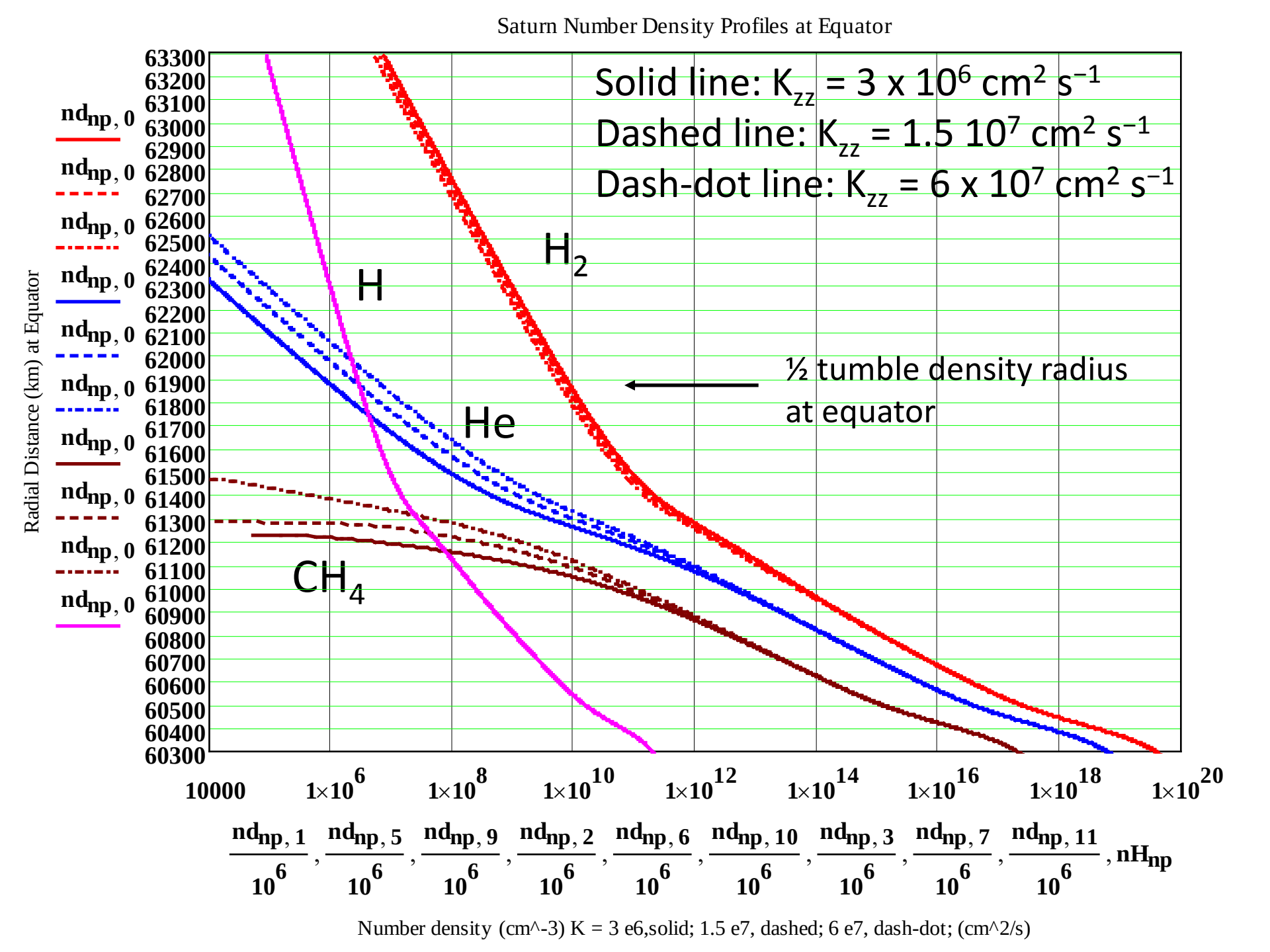
Saturn Number Density Profiles at Equator
Solid line: K_{zz} = 3 x 10^6 cm^2 s^{-1}
Dashed line: K_{zz} = 1.5 10^7 cm^2 s^{-1}
Dash-dot line: K_{zz} = 6 x 10^7 cm^2 s^{-1}
H
H_2
He
CH_4
½ tumble density radius
at equator
Radial Distance (km) at Equator
63300
63200
63100
63000
62900
62800
62700
62600
62500
62400
62300
62200
62100
62000
61900
61800
61700
61600
61500
61400
61300
61200
61100
61000
60900
60800
60700
60600
60500
60400
60300
10000
1×10^6
1×10^8
1×10^{10}
1×10^{12}
1×10^{14}
1×10^{16}
1×10^{18}
1×10^{20}
$\frac{nd_{np,1}}{10^6}$, $\frac{nd_{np,5}}{10^6}$, $\frac{nd_{np,9}}{10^6}$, $\frac{nd_{np,2}}{10^6}$, $\frac{nd_{np,6}}{10^6}$, $\frac{nd_{np,10}}{10^6}$, $\frac{nd_{np,3}}{10^6}$, $\frac{nd_{np,7}}{10^6}$, $\frac{nd_{np,11}}{10^6}$, nH_{np}
Number density (cm^-3) K = 3 e6,solid; 1.5 e7, dashed; 6 e7, dash-dot; (cm^2/s)

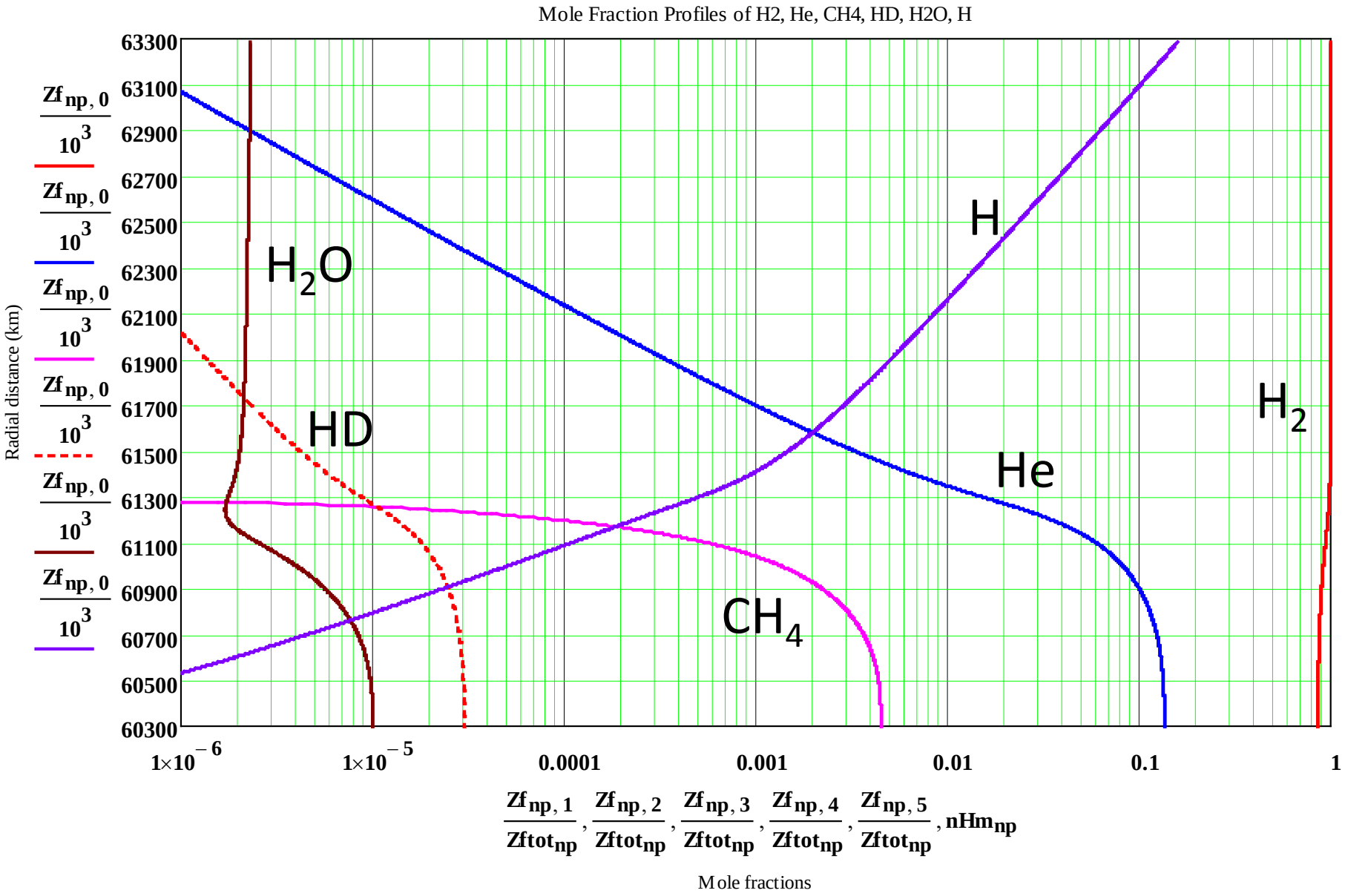

$\phi(H2O) = -2 \times 10^7\ cm^2\ s^{-1}$; $K_{zz} = 1.5\ 10^7\ cm^2\ s^{-1}$

Saturn Thermospheric Airglow

- Airglow is dominated by H_2 electronic bands, the He 58.4 nm line, the H Lyman line series, and H_3^+ near-IR bands.
- It should be kept in mind that calibration in the EUV/FUV had been a long-term problem for space-borne spectrometers. In addition, the low spectral resolution of the Voyager UVSs and “no resolution” of the Pioneer 10 photometer made interpretation of the data difficult.
- Thus one looks to HUT, HST, and UVIS for high spectral resolution, well-calibrated data.

H_2 Electronic Bands

- Surprisingly large H_2 EUV/FUV dayglow intensities observed by Voyager were finally explained by Liu and Dalgarno (1996) as solar-induced H_2 fluorescence which creates a spectrum distinctly different from electron impact on H_2, because most of the fluorescing photons originate from the $B^1\Sigma_u^+$ state in the v = 6 vibrational level and J = 1 rotational level plus photoelectron impact on H_2. The strongest fluorescence is due to the solar Lyman-β line at 102.572 nm, ~14% of the total, which is coincident with the P(1) line of the Lyman 6-0 band at 102.593 nm.

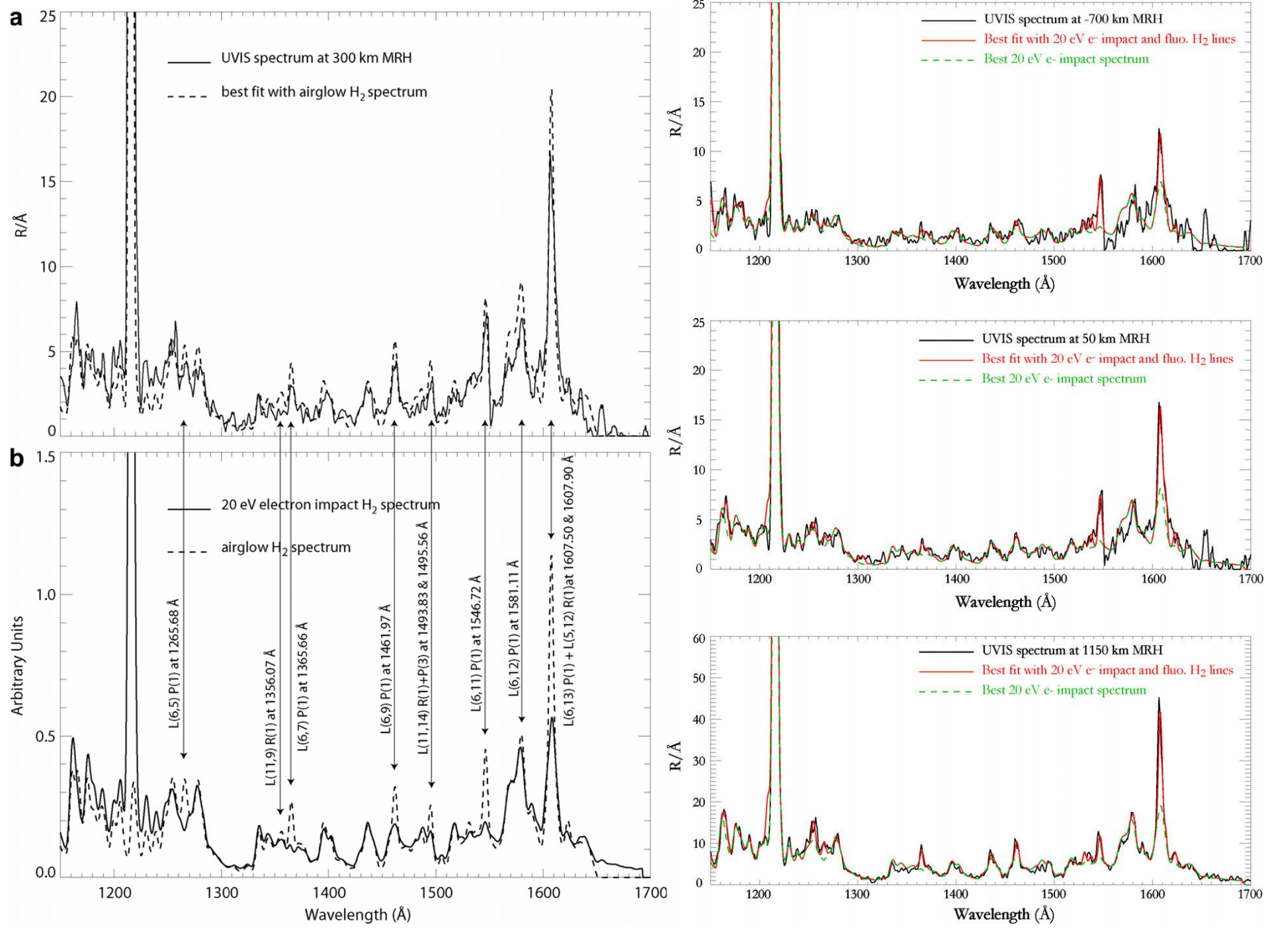
a
UVIS spectrum at 300 km MRH
best fit with airglow H2 spectrum
R/Å
b
20 eV electron impact H2 spectrum
airglow H2 spectrum
Arbitrary Units
L(6,5) P(1) at 1265.68 Å
L(11,9) R(1) at 1356.07 Å
L(6,7) P(1) at 1365.66 Å
L(6,9) P(1) at 1461.97 Å
L(11,14) R(1)+P(3) at 1493.83 & 1495.56 Å
L(6,11) P(1) at 1546.72 Å
L(6,12) P(1) at 1581.11 Å
L(6,13) P(1) + L(5,12) R(1)at 1607.50 & 1607.90 Å
Wavelength (Å)
UVIS spectrum at -700 km MRH
Best fit with 20 eV e- impact and fluo. H2 lines
Best 20 eV e- impact spectrum
R/Å
Wavelength (Å)
UVIS spectrum at 50 km MRH
Best fit with 20 eV e- impact and fluo. H2 lines
Best 20 eV e- impact spectrum
R/Å
Wavelength (Å)
UVIS spectrum at 1150 km MRH
Best fit with 20 eV e- impact and fluo. H2 lines
Best 20 eV e- impact spectrum
R/Å
Wavelength (Å)

Table 2
Characteristics of the main contributions to the airglow emission.

Emission	Peak limb brightness from UVIS (R)[f]	Peak altitude (km)	Main H_2 line contributing	Average brightness from −1200 to 2500 km MRH (R)	Disk values from Liu and Dalgarno (1996) (R)[g]	Peak limb values from V1 and V2 (R)[h]
H Ly-α	802	1100	–	441		V1: 1936, 2543, V2: 1845
L(6, x)[a] P(1) from H Ly-β	120	1000	L(6, 11) P(1) at 1546 Å	42	9.2	
L(11, x)[b] R(1) + P(3) from H Ly-γ	13	750	L(11, 7) P(3) at 1279 Å	6	2.8	
L(2, x)[c] R(4) + P(6) from NII	35	900	L(2, 10) R(4) at 1623 Å	15	3.1	
W(1, x)[d] Q(3) from NII & OVI	26	1250	W(1, 5) Q(3) at 1208 Å	10	2.2	
L(5, x)[e] R(1) + P(3) CII & OVI	60	900	L(5, 11) P(3) at 1613 Å	18	7.1	
1607 Å from H Ly-β, CII & OVI	137	950	L(6, 13) P(1) and L(5, 12) R(1)	33	8.1	
1255 Å mystery feature	18	1200	–	7		
OI triplet	6	−1000	–	4		
Total H_2 bands from e impact	2743	1150	–	1054	131[i]	
Total H_2 bands from fluorescence	1445	900	–	460	173[i]	
Total H_2	3943	1050	–	1514	304[i]	V1: 5386, 4787; V2: 3075

[a] $x = 3, 5, 7, 9, 11, 12, 13, 14$. L stands for Lyman and W for Werner bands.
[b] $x = 5, 7, 9, 10, 14$.
[c] $x = 1, 2, 5, 8, 9, 10$.
[d] $x = 4, 5$.
[e] $x = 3, 5, 6, 8, 10, 12$.
[f] Value deduced from the fits in the 1150–1650 Å bandwidth. The total H_2 value must be multiplied by 1.33 to obtain the total H_2 brightness in the 800–1650 Å range, giving 5244 R. The V1 and V2 limb values in Yelle et al. (1986) refer to "total H_2 bands intensity" without specifying a unambiguous spectral range, which makes it difficult to compare the UVIS and Voyager numbers.
[g] Values from fluorescence lines listed in Table 2 of Liu and Dalgarno (1996), adapted to Saturn at solar minimum. A factor 0.295 is applied to convert the solar irradiance from Jupiter to Saturn and a conversion factor 0.44 is used to account for the solar activity variation between December 1990 (HUT) and November 2005 (UVIS).
[h] Values from Yelle et al. (1986), adapted to November 2005 solar activity. A factor of 0.44 and 0.41 is applied to convert from V1 to UVIS and V2 to UVIS, respectively. Two values are associated with V1 because two limb scans have been performed. The V1 Ly-α values have been multiplied by 0.68 to take into account the UVS damages during the Jupiter encounter (Ben Jaffel et al., 1995).
[i] According to Liu and Dalgarno (1996), the solar fluorescence on Jupiter contributes 57% of the total observed dayglow emission.

H Lyman α 121.6 nm

- Atomic hydrogen above the CH_4 absorbing region can efficiently resonantly scatter the strong solar Lyman-α line, which is broad with a line width of ∼0.1 nm, characteristic of line formation in a region of the solar atmosphere at $\sim 10^{4-5}$ K. The intrinsic planetary line width is determined by thermospheric temperatures, which range from 400 to 550 K. The H column density above the absorbing CH_4 region coupled with the planetary line width determines what fraction of the solar line may be resonantly scattered. While the scattering optical depth at line center can be very large—up to 10^5—it does not extend out to the wings of the solar line, due to the mismatch of line widths indicative of their respective line formation temperatures. This combination of very optically thick at line center and very thin in the wings yields the observed center-to-limb behavior.
- Voyager UVS: 1.5 to 3.3 kR implies H column densities ~ 3-9 x10^{16} cm^{-2} above the absorbing CH_4. Ben Jaffel et al. Icarus, 113,91, 1995 solution was resonance and Rayleigh scattering of solar line ~ -1.5-2.7 kR, ISM ~ 0.45 kR with 3-9 x10^{16} H cm^{-2} ; with only the higher column density yielding > 3 kR
- Gustin et al., Icarus, 210, 270, 2010 give Voyager V1: 1.9, 2.5 kR; V2: 1.8 kR; from UVIS limb scan, the peak brightness is 0.8 kR with average over scan of 0.44 kR.

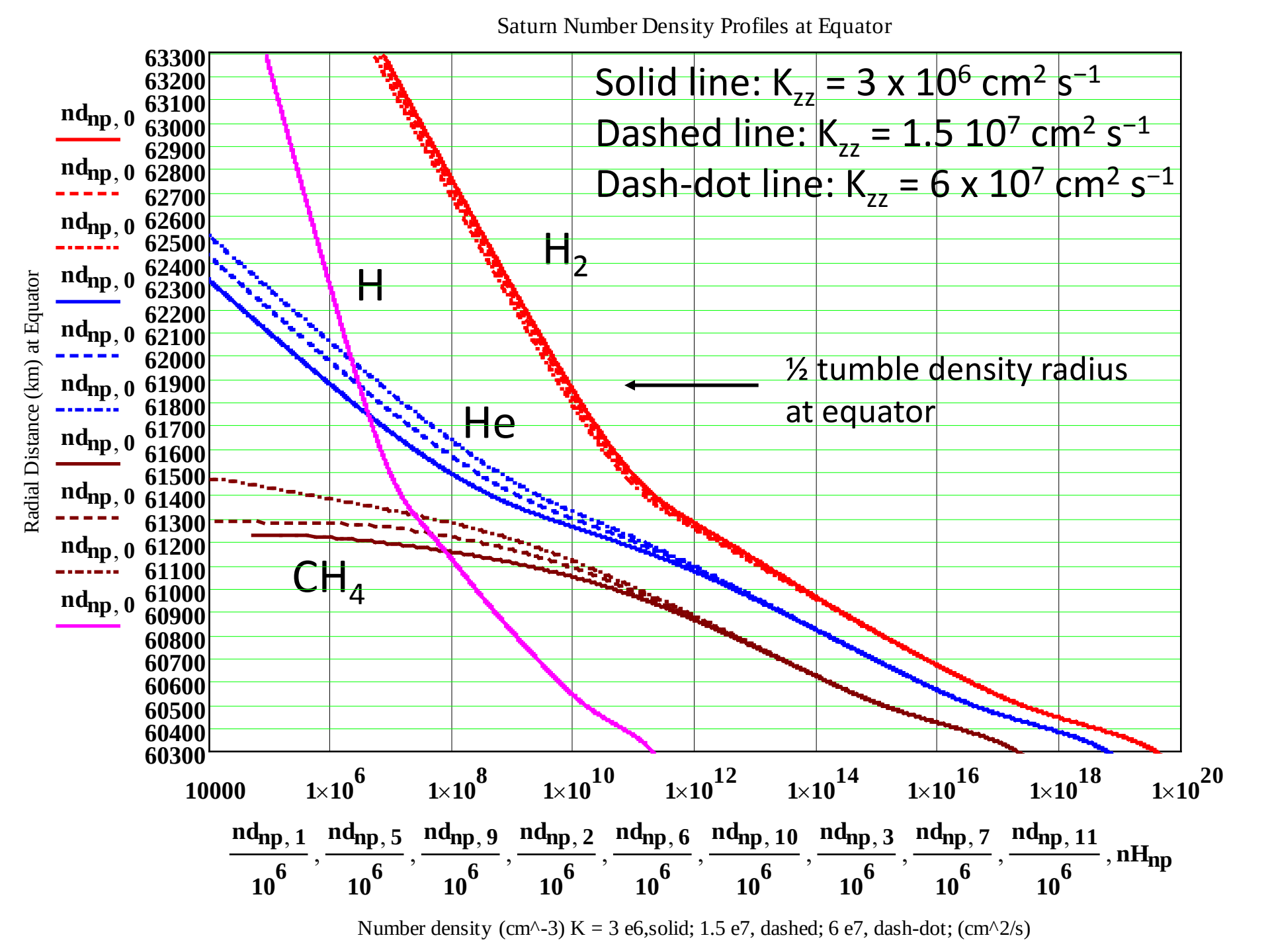
Saturn Number Density Profiles at Equator
Solid line: K_{zz} = 3 x 10^6 cm^2 s^{-1}
Dashed line: K_{zz} = 1.5 10^7 cm^2 s^{-1}
Dash-dot line: K_{zz} = 6 x 10^7 cm^2 s^{-1}
H
H_2
He
CH_4
½ tumble density radius
at equator
Radial Distance (km) at Equator
63300
63200
63100
63000
62900
62800
62700
62600
62500
62400
62300
62200
62100
62000
61900
61800
61700
61600
61500
61400
61300
61200
61100
61000
60900
60800
60700
60600
60500
60400
60300
10000
1×10^6
1×10^8
1×10^{10}
1×10^{12}
1×10^{14}
1×10^{16}
1×10^{18}
1×10^{20}
$\frac{nd_{np,1}}{10^6}$, $\frac{nd_{np,5}}{10^6}$, $\frac{nd_{np,9}}{10^6}$, $\frac{nd_{np,2}}{10^6}$, $\frac{nd_{np,6}}{10^6}$, $\frac{nd_{np,10}}{10^6}$, $\frac{nd_{np,3}}{10^6}$, $\frac{nd_{np,7}}{10^6}$, $\frac{nd_{np,11}}{10^6}$, nH_{np}
Number density (cm^-3) K = 3 e6,solid; 1.5 e7, dashed; 6 e7, dash-dot; (cm^2/s)

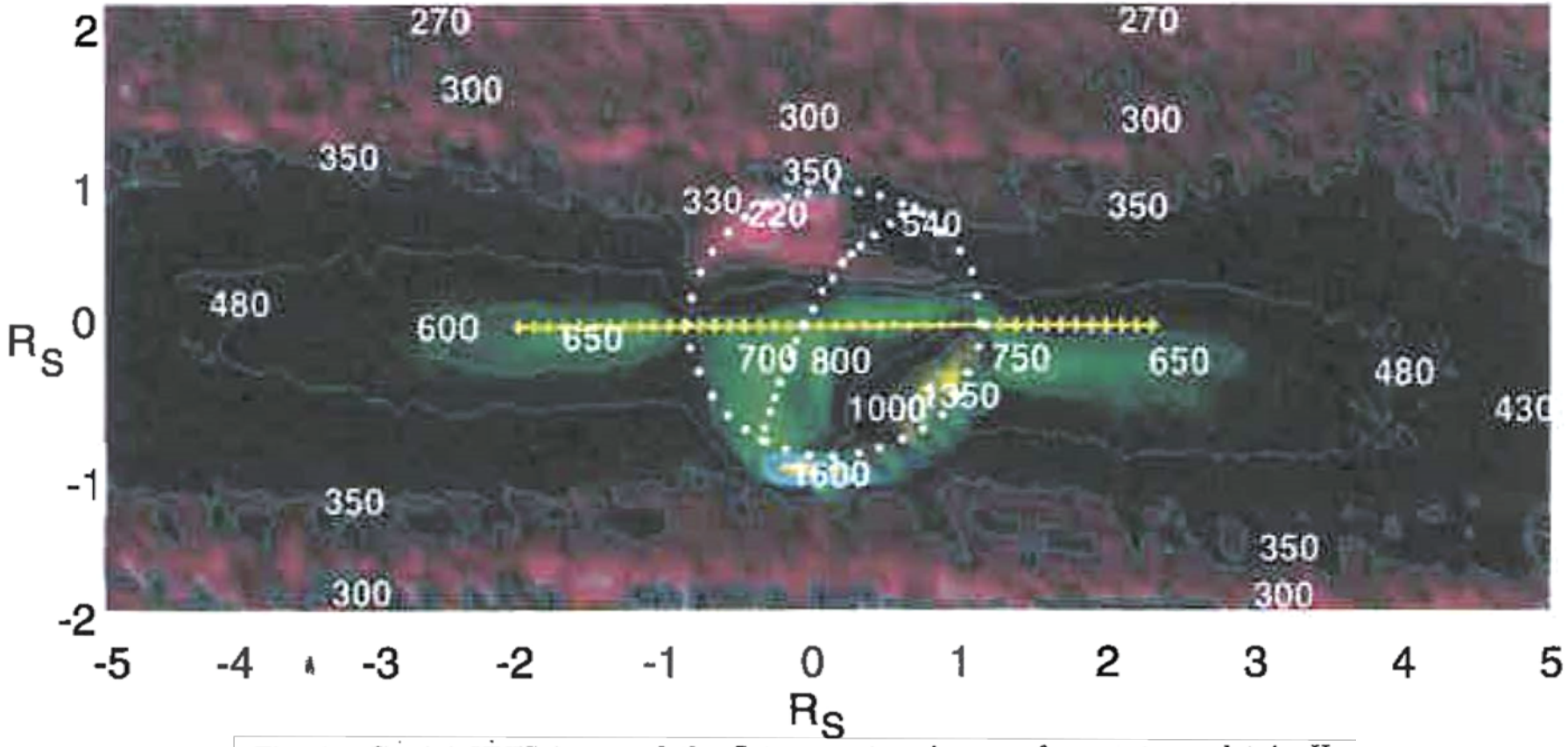

Fig. 1. Cassini UVIS image of the Saturn system in a surface contour plot in H Ly-α emission showing the escape of atomic hydrogen in a non-uniform asymmetric distribution from the top of the Saturn atmosphere. Image accumulated 2005 DOY 74–86 at spacecraft-planet range of 24–44 R_S. The image pixel size is 0.1 × 0.1 R_S. The edge-on view of the rings is indicated; sub-spacecraft latitude is 0°. The 1 bar level and terminator (Sun on right side of image) is indicated by white dots. Range in the virtual image is indicated at the frame of the image in units of R_S, where 0,0 is the position of the planet center. Contour lines of constant brightness are shown on the plot with Rayleigh brightness values given at selected locations. The locally confined emission structure contains a foreground/background signal broadly distributed throughout the magnetosphere with magnitudes indicated near the north and south frames of the image. The core of the plume is at −13.5° planetocentric latitude. Sub-solar latitude is −22.3°. Auroral emission is apparent at the poles extending over the terminator. Solar phase is 77°.

Liu et al. *Advances in Geosciences*, Vol. 19, 2010.

For V2 solar maximum Conditions, Ly-α flux = 6.8 x 10^{11} photons cm^{-2} s^{-1} at 1 AU

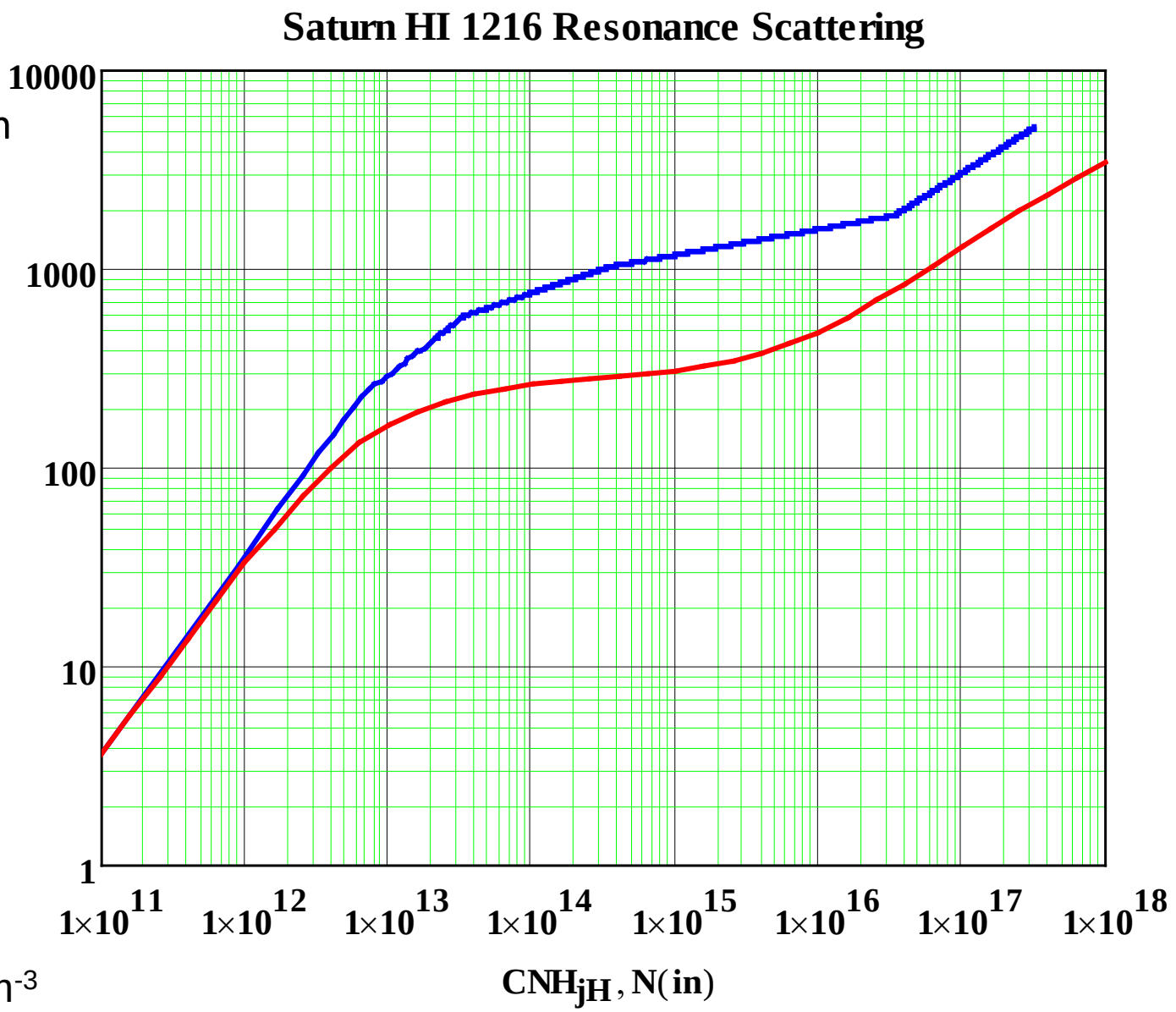

Exobase n(H) = 1 e5 cm^{-3}
Exosphere H column Density = 3.8 e12 cm^{-2}

He 58.4 nm

- The interpretation of the He I 58.4 nm line requires accurate knowledge of the [He]/[H2] ratio, temperature, and vertical mixing at and above the homopause, all uncertain to various degrees. Fundamentally, planetary He absorbs solar He I 58.4 nm radiation and reemits/scatters with a probability equal to 0.9989. The amount of scattering (i.e. brightness) depends on the atmospheric temperature for planetary line width, and the He column density above the unit optical depth due to absorbing H2.
- Voyager UVS V1: 2.2 ± 0.3 R; V2: 4.2 ± 0.5 R (V1: 3.1 ± 0.4 R)
- Parkinson, Ph. D. thesis, York Univ., 2002 performed the most recent analysis of the Saturnian He 58.4 nm line brightness for Voyager UVS. Constrained by Voyager IRIS [He]/[H2] mixing ratio ~ 0.03 and UVS occultation data, he required $K_{zz} > 10^9$ cm^2 s^{-1} and with a solar [He]/[H2] mixing ratio ~ 0.13, $K_{zz} > 2 \times 10^7$ cm^2 s^{-1} for V1 and $K_{zz} > 10^8$ cm^2 s^{-1} for V2.
- Cassini UVIS ??

H_3^+ near-IR bands.

- The H_3^+ ion plays the fundamental role of the thermospheric thermostat for the giant planets in a manner similar to NO in the Earth's thermosphere. The near-IR H_3^+ emissions are the principal means of remotely sensing portions of their ionospheres. The H_3^+ v2 band, between 3.4–4.1 microns, is mostly thermal emission and hence is a measure of the H_3^+ column density and the temperature of the region of the atmosphere where H_3^+ is an abundant ion.
- As it is near-IR emission, elevated temperatures and ionospheric densities are required for detection in the dayglow. From the Wien displacement law, peak blackbody radiation at 4 microns occurs at 750 K and at 1000 K for 3 micron radiation. Saturn's low and mid-latitude thermosphere is colder (~400-500 K) with fewer H_3^+ ions and thus H_3^+ thermal emission can only be detected in hotter (~ 550 K) polar regions.

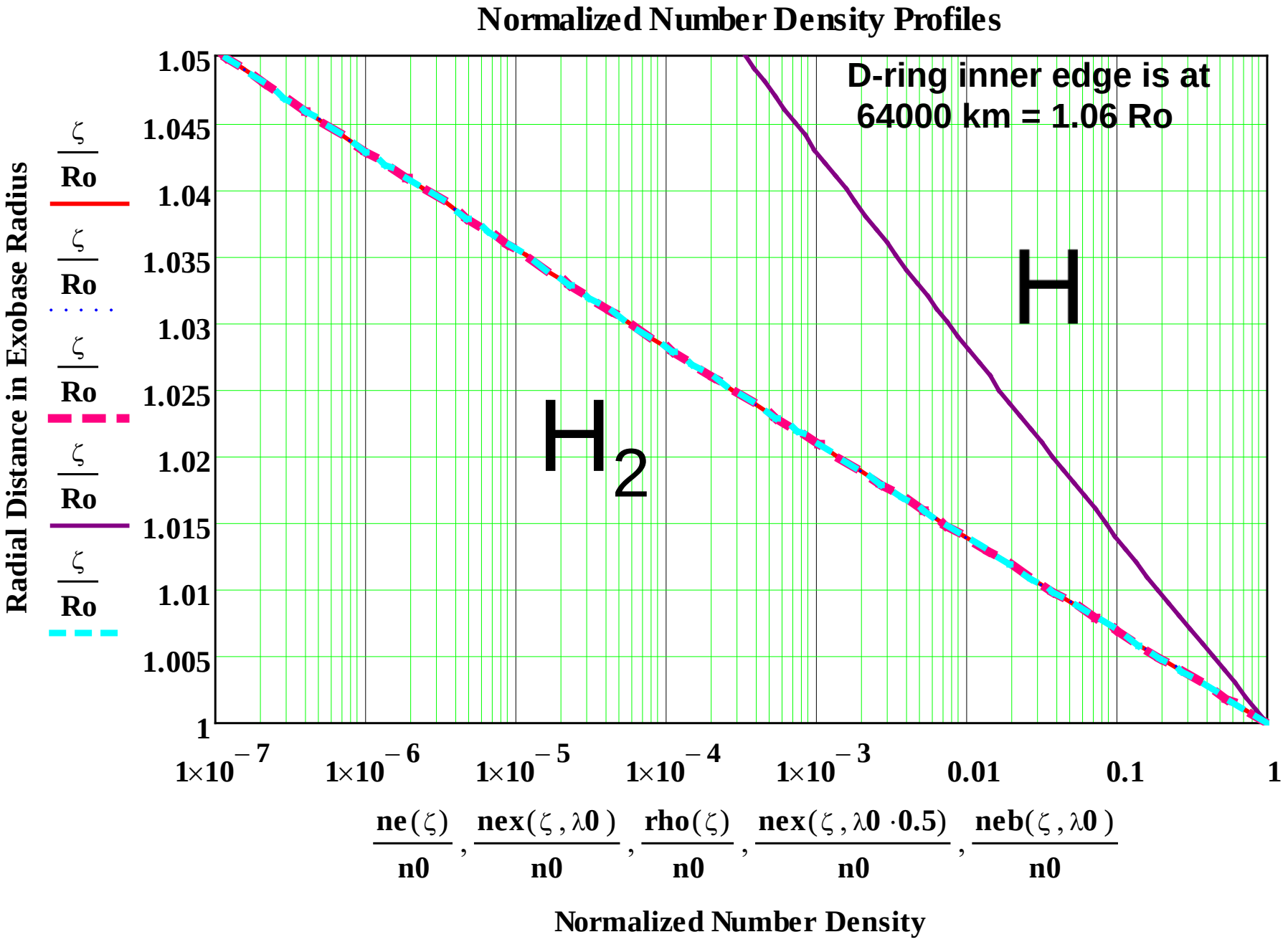
Normalized Number Density Profiles
D-ring inner edge is at
64000 km = 1.06 Ro
H
H2
Radial Distance in Exobase Radius
ζ / Ro
1.05
1.045
1.04
1.035
1.03
1.025
1.02
1.015
1.01
1.005
1
1×10^−7
1×10^−6
1×10^−5
1×10^−4
1×10^−3
0.01
0.1
1
ne(ζ) / n0
nex(ζ, λ0) / n0
rho(ζ) / n0
nex(ζ, λ0 ·0.5) / n0
neb(ζ, λ0) / n0
Normalized Number Density

The Ion Drag Fridge

- Auroral electric fields accelerate ions westward, driving sub-corotation of neutral atmosphere
- Smith et al. (Nature, Jan 2007) showed sub-corotation of thermospheric neutrals at polar latitude would drive a lower altitude equator-to-pole circulation
- This cools the equator
- The stronger auroral forcing, the stronger the sub-corotation and the stronger the equator-to-pole circulation and its cooling effect.
- Does this rule out magnetospheric energy as the solution to the gas giant energy crisis?

The "Ion Drag Fridge"

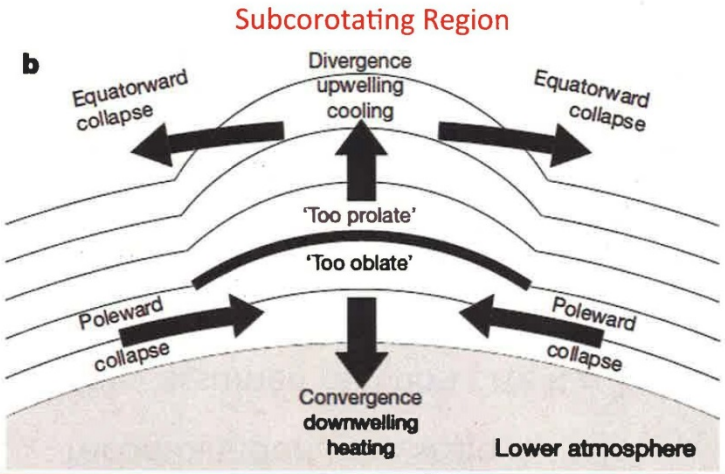

Smith et al., Nature, Jan 2007

Pole-to-equator flow

Equator-to-pole flow

- Polar sub-corotation due to auroral forcing (westward ion velocities due to ambient E fields) drives equator-to-pole circulation
- NOTE: this is not simply the return-flow of thermally driven pole-to-equator winds higher up!
- Therefore, the poleward flow cools the equatorial regions

The End

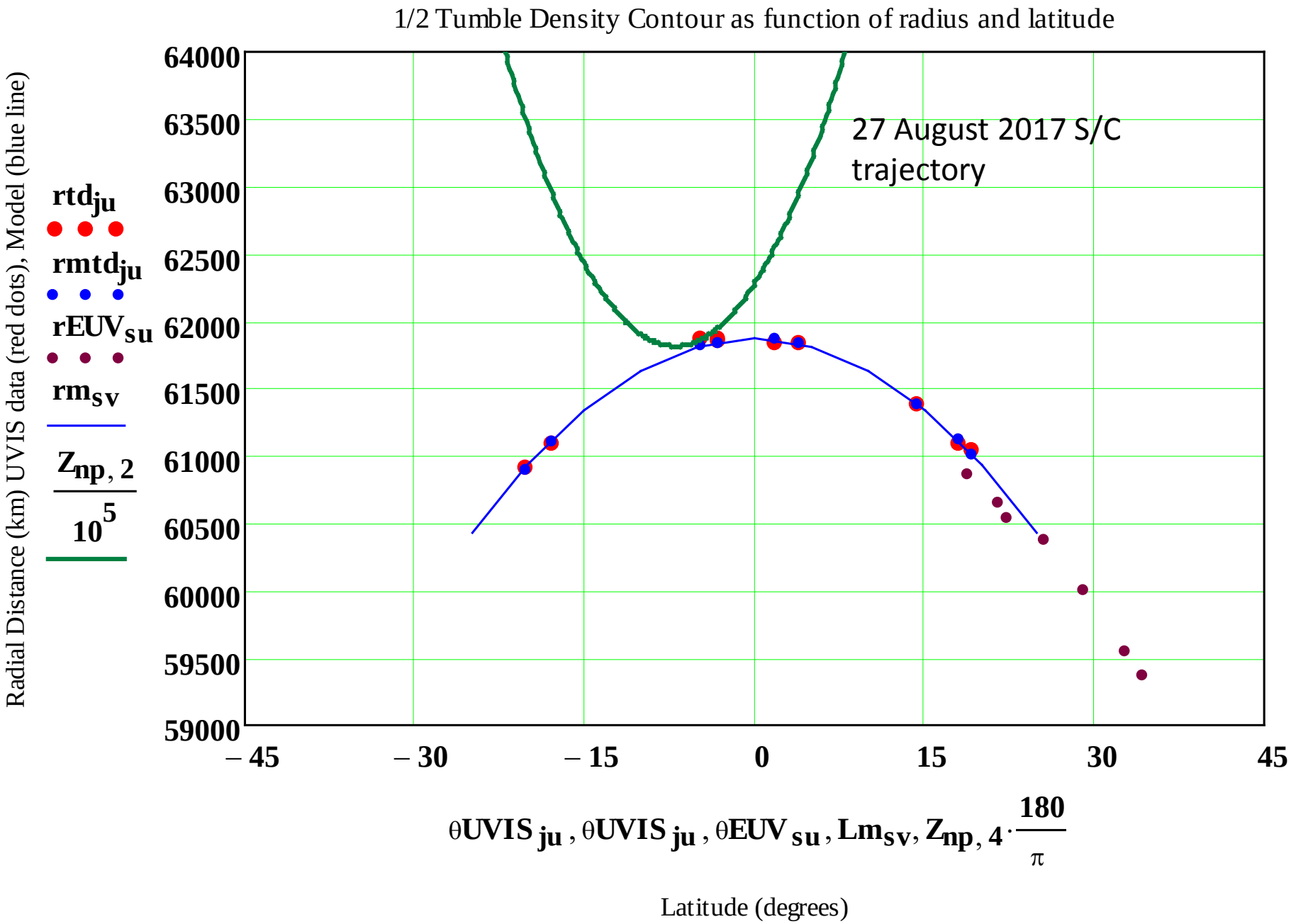

Data points same as slide 3; blue line is ½ tumble density contour; green line S/C trajectory.

Blue line is the nominal adopted "1/2"tumble mass density (2.525 e-11 kg/m^3) model drawn at 5 degree intervals, although the actual tumble density with rotating atmosphere is (8.0 e-11 kg/m^3). Data points from UVIS stellar later (red) and earlier (brown) occultations plus Voyager stellar occultations at nominal ½ tumble density location with the blue points the model location.

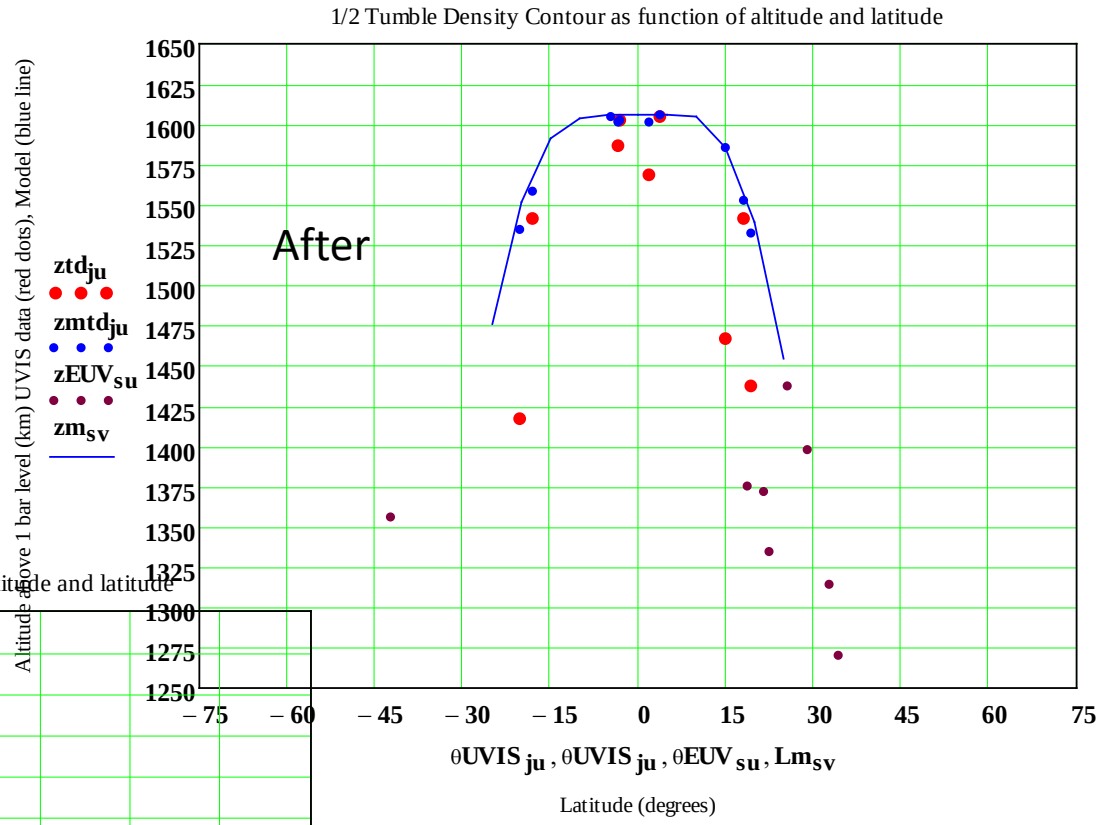

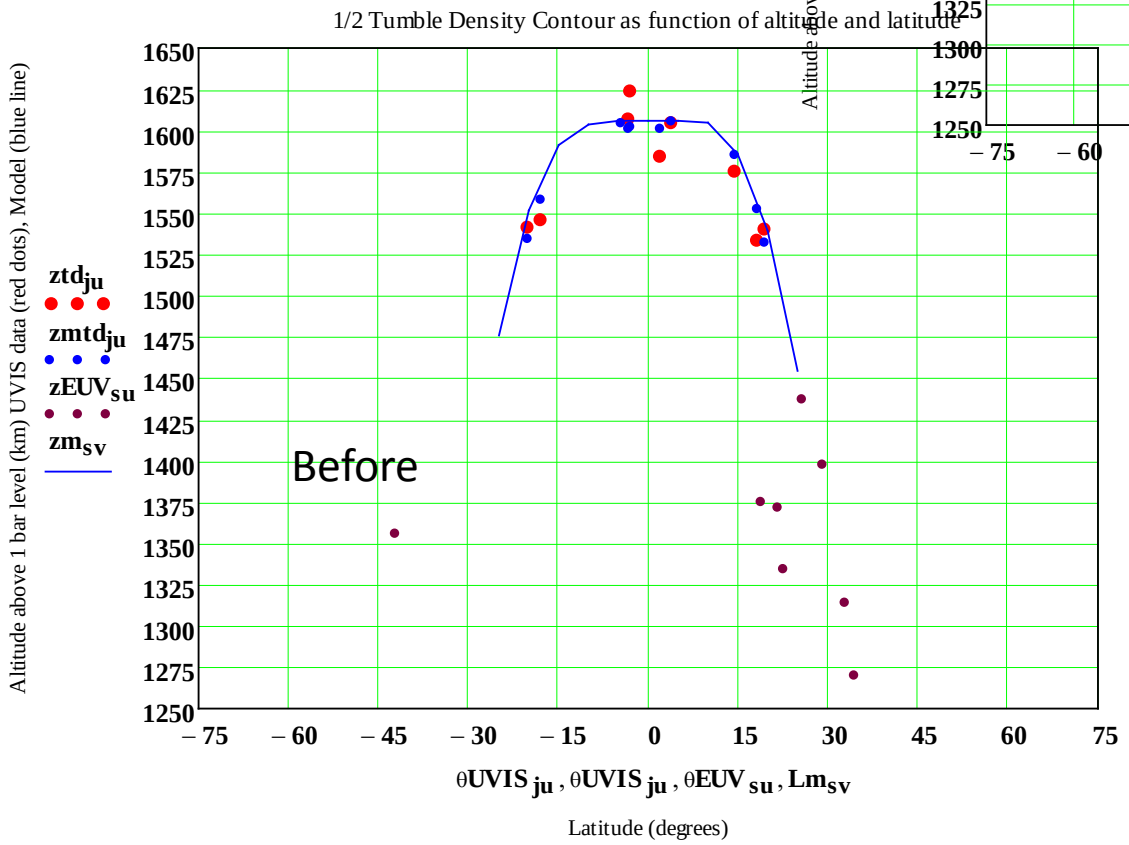

	half tumble density r and z		
Latitude	r (km)	r1bar (km)	z (km)
17.9	61109.43	59567	1542.432
15.05	61219.13	59752	1467.131
1.79	61833.74	60265	1568.74
-3.21	61850.11	60247	1603.108
-3.31	61833.35	60246	1587.348
-17.97	61096.79	59555	1541.79
-20.3	60785.37	59368	1417.375

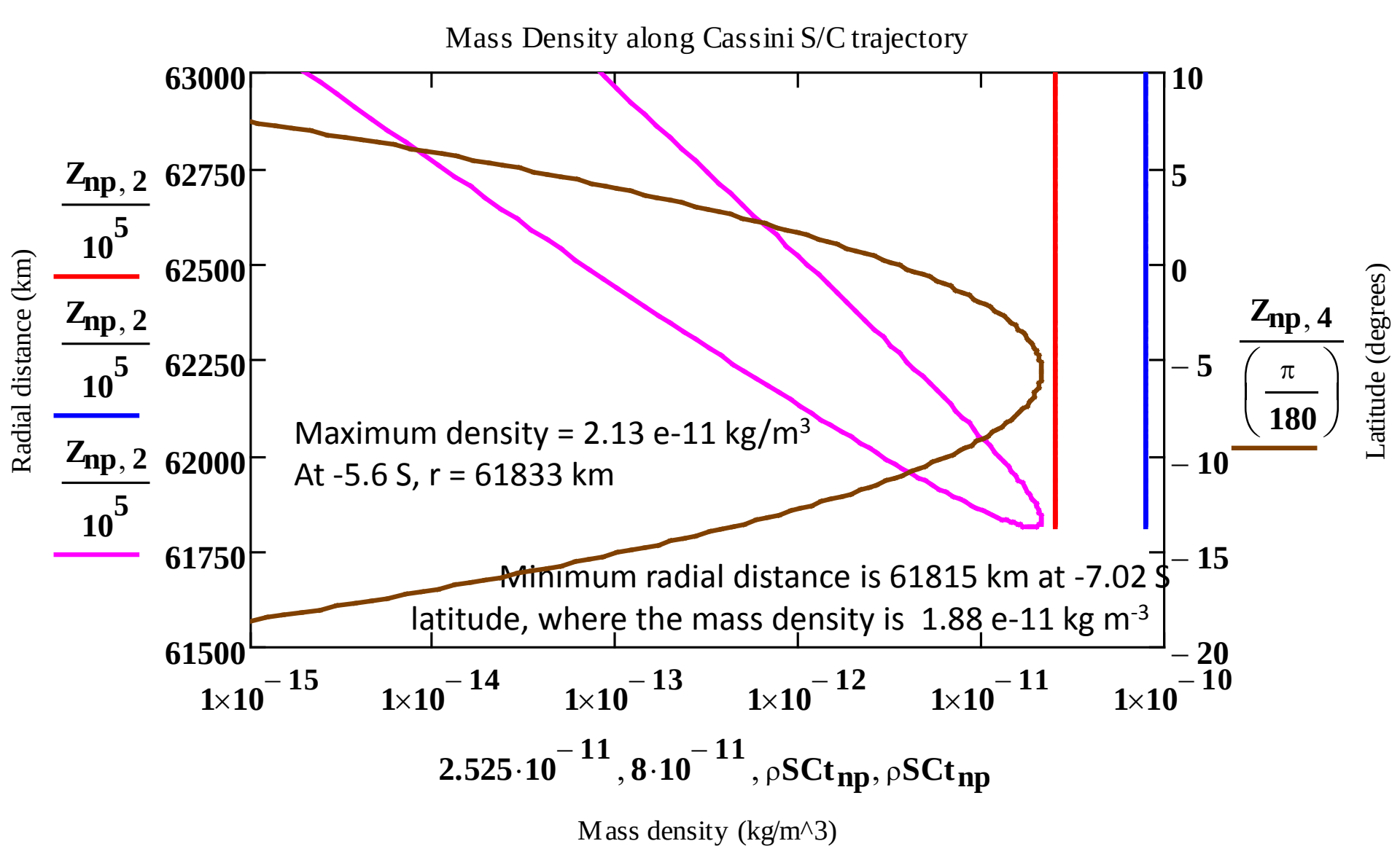

Mass density along S/C trajectory vs radial distance (magenta line) and vs latitude (brown line). Blue line is tumble mass density (8 e-11 kg/m^3) with rotating atmosphere and red line is previous ½ tumble density (2.525 e-11 kg/m^3), which I think is the nominal adopted ½ tumble density.